P H Y S I C A L R E V I E W L E T T E R S

Shearing Active Gels Close to the Isotropic-Nematic Transition

M. E. Cates,[1] S. M. Fielding,[2] D. Marenduzzo,[1] E. Orlandini,[3] and J. M. Yeomans[4]

[1]*SUPA, School of Physics, University of Edinburgh, Edinburgh EH9 3JZ, United Kingdom*
[2]*School of Mathematics and Manchester Centre for Nonlinear Dynamics, University of Manchester,
Manchester M13 9EP, United Kingdom*
[3]*Dipartimento di Fisica, CNISM, and Sezione INFN, Università di Padova, 31121 Padova, Italy*
[4]*The Rudolf Peierls Centre for Theoretical Physics, University of Oxford, Oxford OX1 3NP, United Kingdom*

We study numerically the rheological properties of a slab of active gel close to the isotropic-nematic transition. The flow behavior shows a strong dependence on the sample size, boundary conditions, and on the bulk constitutive curve, which, on entering the nematic phase, acquires an activity-induced discontinuity at the origin. The precursor of this within the metastable isotropic phase for contractile systems (e.g., actomyosin gels) gives a viscosity divergence; its counterpart for extensile suspensions admits instead a shear-banded flow with zero apparent viscosity.

Active gels, including cell extracts and bacterial suspensions, are important and fascinating complex fluids [1–7]. These systems contain self-propelled subunits which, on symmetry grounds, have generic ordering tendencies that favor an isotropic-nematic (I-N) transition. Unlike conventional nematogens, they are driven by a continuous energy flux and remain out of thermodynamic equilibrium even in steady state. Active elements contribute to the stress as force dipoles, characterized as "extensile" or "contractile." Rodlike extensile particles induce a dipolar flow away from their ends round to their long sides, whereas for contractile rods, the flow direction is reversed. This means that an extensile, flow-aligning nematogen placed in a shear flow enhances the applied shear; its contractile counterpart opposes it.

In both cases, the quiescent bulk ordered phase (N) is unstable, but restabilizes at high shear rates [1]. Confining walls can also restore stability [2,7], creating a finite threshold of activity for onset of spontaneous flow. A recent analysis [3] predicts moreover that the zero-shear viscosity of a contractile solution should diverge at the I-N transition. Thereafter, within the N phase, one expects a positive yield stress whose counterpart for an extensile nematic is, however, formally negative [1].

In this Letter, we study numerically the steady states of sheared active gels near the I-N transition. We find shear banding in the extensile case, which replaces a negative-viscosity zone by a window of "superfluidity," accommodating a range of macroscopic shear rates at zero stress. We also find for contractile systems a viscosity divergence [3], at the (spinodal) threshold of the quiescent I-N transition, and discontinuous shear thickening at the shear-induced I-N transition [8]. The slab's dimensions and boundary conditions can strongly influence this strikingly rich range of phenomena.

We hope that, as well as offering insights into the highly nonlinear physics of active gels, our numerics will prompt new rheological experiments on soft active matter such as bacterial suspensions and actomyosin gels.

To gain our results, we used a hybrid lattice Boltzmann (HLB) algorithm [7], whose approximations are shared by the hydrodynamic equations of motion (detailed below) of active fluids [1–3], and also a finite difference (FD) algorithm that additionally neglects inertia [8,9]. We assume translational invariance along flow and vorticity directions, reducing the 3D problem to 1D.

Governing Equations.—In a coarse grained approach, the local properties of an (apolar) active fluid can be described by a tensor order-parameter, $Q_{\alpha\beta}$, whose largest eigenvalue, $2q/3$, and its associated eigenvector give the magnitude and direction of the local orientational order. The equilibrium physics of the passive system is reproduced by a Landau–de Gennes free energy $\mathcal{F}$ with density

$$\left(1 - \frac{\varphi}{3}\right)\frac{Q_{\alpha\beta}^2}{2} - \frac{\varphi}{3}\mathrm{Tr}(Q^3) + \frac{\varphi}{4}(Q_{\alpha\beta}^2)^2 + \frac{K}{2}(\partial_\gamma Q_{\alpha\beta})^2 \tag{1}$$

where φ controls the magnitude of the ordering. There is a first order transition between the N phase, stable for $\varphi > 2.7$ and the I phase, stable for $\varphi < 2.7$. At $\varphi = 3.0$ lies the spinodal point, the limit of the metastability of the I phase. In the last term of (1) K is an elastic constant [10]. The equation of motion for $Q_{\alpha\beta}$ is [11] $D_t Q_{\alpha\beta} = \Gamma H_{\alpha\beta}$ with D_t a material derivative describing advection by the fluid velocity u_α, and rotation/stretch by flow gradients (see [7,11]). The molecular field is $H_{\alpha\beta} = -\frac{\delta\mathcal{F}}{\delta Q_{\alpha\beta}} + (\delta_{\alpha\beta}/3)\mathrm{Tr}\frac{\delta\mathcal{F}}{\delta Q_{\alpha\beta}}$, and Γ is a collective rotational diffusivity. Flow is governed by the continuity and Navier Stokes equations for a Newtonian fluid of density ρ and viscosity η, forced by an order-parameter stress

$$
\Pi_{\alpha\beta} = 2\xi\left(Q_{\alpha\beta} + \frac{1}{3}\delta_{\alpha\beta}\right)Q_{\gamma\epsilon}H_{\gamma\epsilon} - \xi H_{\alpha\gamma}\left(Q_{\gamma\beta} + \frac{1}{3}\delta_{\gamma\beta}\right)
$$
$$
- \xi\left(Q_{\alpha\gamma} + \frac{1}{3}\delta_{\alpha\gamma}\right)H_{\gamma\beta} - \partial_\alpha Q_{\gamma\nu}\frac{\delta\mathcal{F}}{\delta\partial_\beta Q_{\gamma\nu}}
$$
$$
+ Q_{\alpha\gamma}H_{\gamma\beta} - H_{\alpha\gamma}Q_{\gamma\beta} - \zeta Q_{\alpha\beta}. \qquad (2)
$$

The last term of (2) stems from activity, with $\zeta > 0$ (extensile) or $\zeta < 0$ (contractile) [1–3,7]. The parameter ξ depends on the geometry of active elements; it determines whether the material is flow-aligning or flow-tumbling. We restrict ourselves to the former by taking $\xi = 0.7$ (representative of a gel in the aligning regime). Our equations describe for simplicity apolar active gels, whereas many such gels (e.g., actomysin) are polar [12].

Constitutive Curves.—We first compute [13] curves $\sigma(\dot{\gamma})$ for the shear stress σ at uniform imposed shear rate $\dot{\gamma} \equiv \partial_y u_x$. Figure 1 shows this curve (and its stress contributions) for an extensile nematic. With our parameters, the passive terms in Π_{xy} are much smaller than the viscous stress $\eta\dot{\gamma}$, so $\sigma \simeq \eta\dot{\gamma} - \zeta Q_{xy}(\dot{\gamma})$. In flow-aligning nematics, Q_{xy} has an upward discontinuity at the origin (see Fig. 1); for contractile materials ($\zeta < 0$), this creates an upward step in $\sigma(\dot{\gamma})$, or yield stress [1]. The constitutive curve for the extensile case ($\zeta > 0$, Fig. 1) instead has a downward step, or "negative yield stress," causing a zone of negative viscosity ($\sigma/\dot{\gamma} < 0$) for $|\dot{\gamma}| < \dot{\gamma}^*$, which can be circumvented by splitting into shear bands of $\dot{\gamma} = \pm\dot{\gamma}^*$. The resulting composite flow curve $\sigma(\dot{\gamma})$, with $\dot{\gamma}$ now the applied (mean) shear rate, connects $\dot{\gamma} = \pm\dot{\gamma}^*$ with a horizontal "tie line" at zero stress. The stability of such bands is far from certain; however, our FD work (data not shown) confirms the existence of such states in the 1D bulk (large L) limit. Figures 5–7 of [7] on confined slabs also offer evidence for this N/N banding scenario which, we argue

below, should also control flow of extensile systems initialized in the I phase close the I-N spinodal.

Slab Geometry.—We next consider a slab of active gel between parallel plates at y-separation L, with x-velocities $\pm\dot{\gamma}L/2$. Our main HLB runs have $L = 100$, $\Gamma = 0.33775$, $K = 0.04$, $\eta = 5/3$, $\rho = 2$, and $\zeta = \pm0.005$. These values, and our results, are reported in LB units; such units map, e.g., to $\Delta x = 0.05 \ \mu$m and $\Delta t = 0.67 \ \mu$s with $\Gamma = 1$ Poise, $\eta = 1.1$ Poise, $K = 10$ pN [10], and $\zeta = 500$ Pa. The only length scale in Eqs. (1) and (2) is then $\ell \equiv K^{1/2} \simeq 5$ nm. These represent molecular nematogens in a microfluidic-device-scale slab ($L \sim 5 \ \mu$m) [7]; very different values might arise in some biological contexts.

Below we compare "fixed" (anchored) boundary conditions, in which $Q_{\alpha\beta}$ is specified on the walls, and "free" ones which effectively set $\partial_y Q_{\alpha\beta} = 0$, at $y = 0$, L. For shear-banding problems, the latter choice promotes convergence to bulk behavior [14]; our FD work uses this, and to the same end, chooses small $\ell/L = 5 \times 10^{-4}$. The boundary condition on u_α is taken as no-slip.

Linear Contractile Rheology.—We now report apparent viscosities $\eta_{app}(\dot{\gamma}, L, \ldots) = (\Pi_{xy} + \eta\partial_y u_x)/\dot{\gamma}$. For homogeneous flows, these give the bulk flow curve $\eta_{app} = \sigma(\dot{\gamma})/\dot{\gamma}$ and reduce to the zero-shear viscosity as $\dot{\gamma} \to 0$.

We start with the zero-shear viscosity of a contractile gel in the metastable I phase, $2.7 < \varphi \leq 3.0$. We observe a viscosity divergence at the latter (spinodal) point, as predicted in [3] (this addressed 2D nematogens for which binodal and spinodal coincide). This is shown in Fig. 2(a), where the divergence is seen with free-boundary conditions, for which the flow remains homogeneous, but is suppressed if $Q_{\alpha\beta}$ is anchored at the walls with director along the flow (creating nonuniform shear there). In the latter case, η_{app} increases linearly with L (we have simulated up to $L = 400$) until it saturates, for $\varphi < 3$, at the free-boundary value. To understand this, note that surface anchoring lifts the rotational degeneracy of the N phase, so that deviations of the director **n** away from x feel a finite
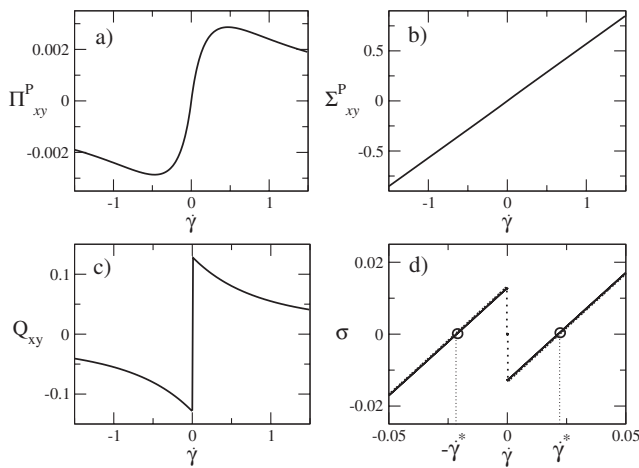

FIG. 1. For an extensile nematic ($\varphi = 3.0$, $\xi = 0.7$, $\eta = 0.567$, $\zeta = 0.1$), as functions of $\dot{\gamma}$ in steady state :(a) Passive order-parameter stress $\Pi^P_{xy} = \Pi_{xy} + \zeta Q_{xy}$; (b) Total passive stress $\Sigma^P_{xy} = \Pi^P_{xy} + \eta\dot{\gamma}$; (c) Order-parameter Q_{xy}; (d) Total shear stress $\sigma(\dot{\gamma})$ (dotted curve: the same for $\varphi = 2.95$).
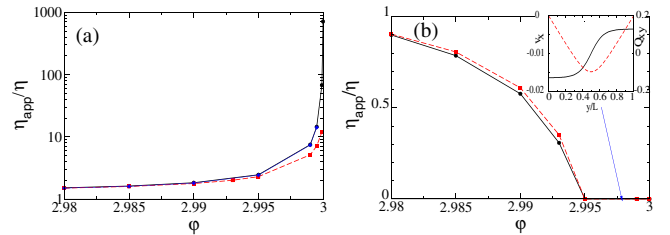

FIG. 2 (color online). (a) Apparent zero shear viscosity for an isotropic contractile gel in a slab under shear. Solid curve(s): free-boundary conditions; HLB data are indistinguishable from those derived from the bulk flow curve [13]. Dashed curve: fixed boundaries (director along flow). (b) Apparent viscosity in a linear regime for an active extensile gel in a slab under shear. Solid and dashed curves correspond to systems with free and fixed boundaries, respectively. The insets show plots of Q_{xy} and u_x (solid and dashed lines) in the $\eta_{app} = 0$ phase.

restoring force (for $L < \infty$). Hence, the active shear stress, $\sim -\zeta q n_x n_y$, remains of order $\dot{\gamma}$, and there can be no yield stress, nor any viscosity divergence.

Extensile Rheology.—Consider next systems initialized in the metastable I phase of an extensile material ($\zeta = 0.005$). These have strikingly different behaviors, shown in Fig. 2(b). Not only does η_{app} decrease strongly as the spinodal is approached: it becomes strictly zero in an interval $\varphi_c(\zeta, L) < \varphi < 3$. We argue that this "superfluid" window replaces one of negative viscosity on the constitutive curve, arising for $\varphi > \varphi^*(\zeta)$ (say), and similar to that already discussed for extensile nematic phases (Fig. 1). To understand its continued presence here, note that as $\varphi \to 3^-$ and at $\dot{\gamma} = 0$, $\partial Q_{xy}/\partial \dot{\gamma} \to -\infty$; hence, at small $|\dot{\gamma}|$, the flow curve has large negative slope. As $|\dot{\gamma}|$ increases, nonmonotonic features can arise, but the flow curve then joins that of the nematic, before stability is restored at $|\dot{\gamma}| = \dot{\gamma}^*$. Close enough to the spinodal, therefore, the flow curve of the metastable I phase still has all the features needed for formation of bulk N/N shear bands. We then expect $\varphi_c(\zeta, L \to \infty) = \varphi^*(\zeta)$; this is numerically consistent with our HLB and FD data.

However, bulk shear bands do not provide a complete picture for the confined slab of Fig. 2(b), where Q_{xy} and u_x remain relatively smooth on the scale of L (inset). With fixed boundary conditions, the zero-viscosity window is narrower and can disappear at small L. A complementary interpretation of our N/N-banded state is as a "spontaneous flow" phase, predicted inside the nematic region of confined extensile materials [2,7]. Our simulations indicate that, on increasing φ, a direct transition from metastable I to the flow phase is possible.

Nonlinear Contractile Rheology.—We again focus on the metastable I regime, $2.7 < \varphi \leq 3.0$, whose passive counterpart shows shear thinning, and a shear-induced I-N transition [11]. In Fig. 3, we plot HLB results for $\eta_{\text{app}}(\dot{\gamma})$ in a confined slab of a contractile gel, with each shear rate $\dot{\gamma}$ initiated from rest [15]. Consider first the solid line, for $\varphi = 2.99$, with an initially isotropic state, and fixed $Q_{\alpha\beta} = 0$ on the walls. For small $\dot{\gamma}$, there is a linear regime of constant viscosity; the material remains in the I phase. There is then a sharp increase in η_{app}, i.e., strong shear thickening (discontinuous at large L/ℓ), with onset of nematic order oriented near but above the Leslie angle $\theta = \theta^*$, and a drastically non-Newtonian flow profile (Fig. 3, inset). At larger $\dot{\gamma}$, θ decreases and η_{app} falls towards η. The dashed curve shows the same system but with fixed nematic ordering and $\mathbf{n} \parallel \hat{\mathbf{x}}$ at the walls. For small $\dot{\gamma}$, the shear flow is now mainly confined to wall layers; the director has $\theta \simeq 0$ throughout the slab. In the wall layers, the backflow term $\Pi_{\alpha\beta}$ acts to restore the ordering, creating extra dissipation and enhanced η_{app} at small $\dot{\gamma}$. (This scenario is reminiscent of a passive nematogen flowing in the permeation mode close to the isotropic-cholesteric transition [16], where energy from the applied shear is converted into a flow that opposes the shear and reduces
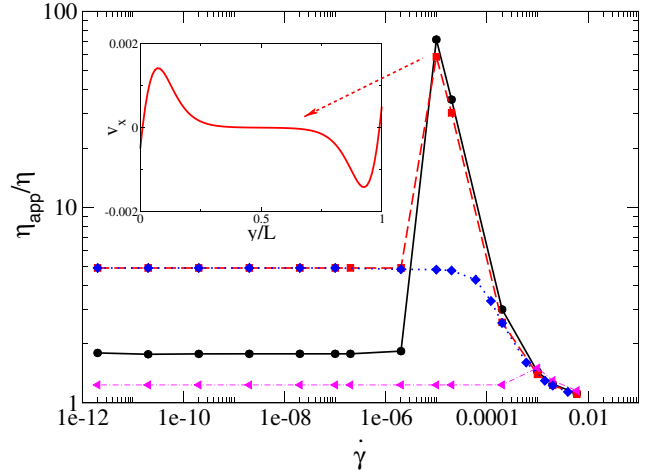

FIG. 3 (color online). η_{app} vs $\dot{\gamma}$ for $\varphi = 2.99$ (solid, dashed, and dotted lines) and $\varphi = 2.8$ (dot-dashed line) for contractile gels under shear. Anchored BCs are considered, with $Q_{\alpha\beta} = 0$ (solid, dot-dashed lines) or with $\mathbf{n} \parallel \hat{\mathbf{x}}$ (long-dashed and dotted lines). For the dotted line, the bulk was initialized with nematic order.

the order.) Shear thickening is now accompanied by an abrupt director transition, near the slab center. As $\dot{\gamma}$ is raised, θ decreases, η_{app} falls, and a Newtonian flow profile is restored. If, instead, the system is initialized in the nematic phase (dotted curve) the jump in θ disappears, as does the peak in η_{app}. Finally, we consider an initial I state further from the spinodal at $\varphi = 2.8$, with $Q_{\alpha\beta} = 0$ at the wall (dot-dashed line). This system remains isotropic for longer: η_{app} is smaller in the linear regime, remains there to higher $\dot{\gamma}$, and shows a smaller peak at the shear-induced I-N transition.
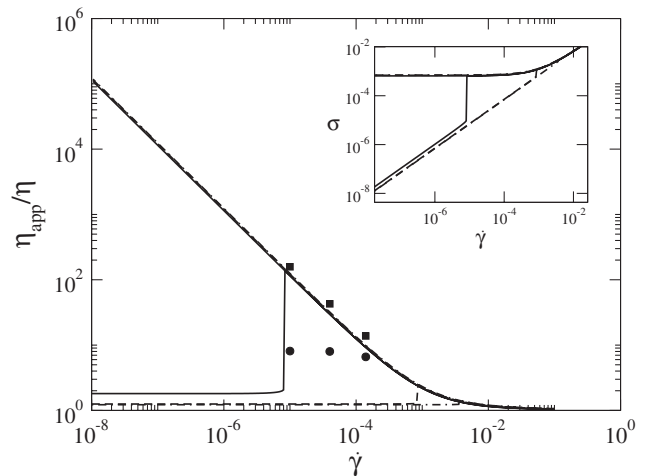

FIG. 4. Viscosity and (inset) flow curves for active contractile gels in bulk homogeneous shear: $\varphi = 2.8, 2.9, 2.99$ (dot-dashed, dashed, solid lines). Vertical line segments signify the end of the I branch and a jump up to N. Data with nematic anchoring as in Fig. 3 are shown for an initially isotropic (squares) or nematic (circles) bulk.
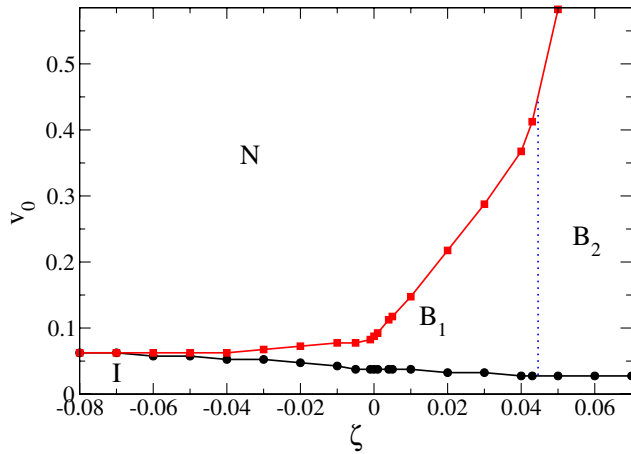
FIG. 5 (color online). Dynamic phase diagram in the (ζ, v_0) plane (with $v_0 = \dot{\gamma}L$ the wall velocity; $L = 100$) for an active liquid crystal close to the isotropic-nematic transition ($\varphi = 2.695$, $\eta = 0.28$). The phases are labeled as follows: N = nematic, I = isotropic, B1 = I/N banded, B2 = N/N banded.

These results for confined slabs are again illuminated by computing the homogeneous bulk flow curve $\sigma(\dot{\gamma})$ [13]. For $\zeta < 0$, this has a low viscosity I branch, terminating at some finite flow rate, and a high viscosity, shear thinning N branch (reflecting a yield stress). Figure 4 shows both the flow curves (inset) and the viscosity $\eta(\dot{\gamma})$. Discontinuous shear-thickening arises on tracking up to the end of the I branch, then jumping vertically to N. (On decreasing shear rate, N can be tracked downwards to low $\dot{\gamma}$ and likely remains metastable.) Again, there are features of the confined behavior, such as boundary-condition sensitivity, that this bulk picture cannot explain.

We finally consider the effect of activity on the I/N shear banding present already in passive nematogens [8]. To this end, we fix $\varphi = 2.695$ and $K = 0.01$; in the passive system ($\zeta = 0$), there is a range of shear rates $\dot{\gamma}$ for which the fluid splits into I and N bands of high and low viscosity. Activity has a significant impact: as shown in Fig. 5, it widens or narrows the banding window according to the sign of ζ. (For larger φ, the bands pinch off giving a direct I/N transition, as reported above, in sufficiently contractile materials.) The trend concurs with expectations from the bulk flow curve: $\sigma(\dot{\gamma})$ for the N phase is lowered by extensile and raised by contractile activity, allowing the former system to band more easily.

To conclude, we have studied an active nematogen close to the I-N transition subjected to a shear flow, assuming translational invariance along flow and vorticity directions. For contractile gels and free-boundary conditions, there is a divergence of the apparent viscosity at the I-N spinodal [3]. Extensile gels, in contrast, enter a zero-viscosity phase of N/N shear bands as the spinodal is approached. In the nonlinear regime, both extensile and contractile materials

show nonmonotonic effective flow curves, with details strongly dependent on initial and boundary conditions. Finally, extensile (contractile) activity stabilizes (suppresses) I/N shear banding. We hope our results will spur experimental investigations of the rheology of active gels, such as extensile bacterial suspensions, or semidilute contractile actomyosin or kinesin-microtubule solutions.

[1] R. A. Simha and S. Ramaswamy, Phys. Rev. Lett. **89,** 058101 (2002); Y. Hatwalne *et al.*, Phys. Rev. Lett. **92,** 118101 (2004); V. Narayan, S. Ramaswamy, and N. Menon, Science **317,** 105 (2007); S. Muhuri, M. Rao, and S. Ramaswamy, Europhys. Lett. **78,** 48002 (2007).

[2] K. Kruse *et al.*, Eur. Phys. J. E **16,** 5 (2005); K. Kruse *et al.*, Phys. Rev. Lett. **92,** 078101 (2004); R. Voituriez, J. F. Joanny, and J. Prost, Europhys. Lett. **70,** 404 (2005); Phys. Rev. Lett. **96,** 028102 (2006).

[3] T. B. Liverpool and M. C. Marchetti, Phys. Rev. Lett. **97,** 268101 (2006); Phys. Rev. Lett. **90,** 138102 (2003); Europhys. Lett. **69,** 846 (2005).

[4] I. Llopis and I. Pagonabarraga, Europhys. Lett. **75,** 999 (2006); S. Ramachandran, P. B. S. Kumar, and I. Pagonabarraga, Eur. Phys. J. E **20,** 151 (2006).

[5] I. S. Aranson *et al.*, Phys. Rev. E **75,** 040901(R) (2007); C. Dombrowski *et al.*, Phys. Rev. Lett. **93,** 098103 (2004).

[6] D. Bray, *Cell Movements: From Molecules To Motility* (Garland Publishing, New York, 2000); D. Humphrey *et al.*, Nature (London) **416,** 413 (2002); F. J. Nedelec *et al.*, Nature (London) **389,** 305 (1997).

[7] D. Marenduzzo, E. Orlandini, and J. M. Yeomans, Phys. Rev. Lett. **98,** 118102 (2007); D. Marenduzzo, E. Orlandini, M. E. Cates, and J. M. Yeomans, Phys. Rev. E **76,** 031921 (2007); J. Non-Newtonian Fluid Mech. **149,** 56 (2008).

[8] S. M. Fielding and P. D. Olmsted, Phys. Rev. Lett. **92,** 084502 (2004).

[9] S. M. Fielding, Phys. Rev. E **77,** 021504 (2008).

[10] P. G. de Gennes and J. Prost, *The Physics of Liquid Crystals* (Clarendon Press, Oxford, 1993), 2nd ed..

[11] A. N. Beris and B. J. Edwards, *Thermodynamics of Flowing Systems* (Oxford University Press, Oxford, 1994).

[12] While the active stress has the same form for polar and apolar gels [1], polarity leads to self-advection of the particle with respect to the fluid, and this may yield different results according to the boundary conditions.

[13] $\sigma(\dot{\gamma})$ for putative homogeneous bulk flow was found by Euler time integration with no spatial coordinates.

[14] J. M. Adams, S. M. Fielding, and P. D. Olmsted, J. Non-Newtonian Fluid Mech. (to be published).

[15] The nonlinear rheology of active aligning gels also leads to nonmonotonic viscosity-shear rate curves, with η_{app} decreasing for intermediate values of the shear.

[16] D. Marenduzzo, E. Orlandini, and J. M. Yeomans, Phys. Rev. Lett. **92,** 188301 (2004).